Combined High-Resolution Imaging and Spectroscopy System
A Versatile and Multi-modal Metrology Platform

Tobias Hegemann, Fabian Bürger and Josef Pauli

Intelligent Systems Group, University of Duisburg-Essen, Bismarckstraße 90, 47057 Duisburg, Duisburg, Germany

Keywords: Imaging, Spectroscopy, Surface Analysis, Metrology, Calibration.

Abstract: Multi- and hyperspectral measurement methods are a versatile approach to analyzing and understanding material properties. Especially imaging techniques allow for a precise sensing of surface properties. This paper presents a novel and multi-purpose metrology platform for high-resolution spectral measurements. The system is able to acquire multispectral images with six different spectral channels as well as hyperspectral point measurements and images. This is realized with a combined measurement head that includes a gray value camera as well as two spectrometers ranging from 190*nm* to 1,700*nm*. A three axis Cartesian robot with nanometer-precision allows the analysis of large samples with a size up to $40 \times 10 \times 10$ *cm* and a weight of up to 25*kg*. Approaches to automatically focus both the camera and the spectrometers are presented. The calibration process between the camera and the spectrometers, which is necessary to acquire the full spectral information corresponding to each pixel of the camera image, is described. Example images and measurements are discussed to show the potential of the metrology platform.

1 INTRODUCTION

The analysis of a wider range of the electromagnetic spectrum offers the chance to obtain more information about materials and the quality of samples. To this effect a unique measurement system was built, the flexible and multi-modal metrology platform CHRISS: Combined High-Resolution Imaging and Spectroscopy System. CHRISS allows for multi- and hyperspectral material analysis which offers more information than color images and may be employed in various application fields such as industrial inspection, defect detection, material classification or food quality, but also in medical contexts such as tumor identification (Panasyuk et al., 2007). By analyzing materials with respect to their properties in the electromagnetic spectrum, it is possible to differentiate between substances, learn about the composition of materials in a sample or evaluate the heterogeneity of a specimen. This provides challenges concerning both hardware, as specialized equipment is needed, and software. CHRISS is built to comply with the hardware challenges, and software solutions were implemented to enable autofocusing both camera and spectrometer unit as well as providing interaction between those two units. This paper is organized as follows: In section 2, spectroscopy in its different types is presented, followed by an overview of the developed system in section 3 and an outline of the combined measurement head of camera and spectrometer unit in section 4. In section 5, the autofocus of the camera and the spectrometer unit as well as the calibration between the two units is explained. The paper is concluded with a brief discussion of this work and a notion of future work is given.

2 ESTABLISHED MEASUREMENT PRINCIPLES

Spectroscopy is the study of the interaction between matter and electromagnetic radiation (Skoog and West, 1980). While there are other types of spectroscopy such as vibrational (Long, 1977) and emission spectroscopy (Radziemski and Cremers, 2006), this paper discusses reflectance spectroscopy (Kortüm, 2012) since this type is used in the presented measurement system. Reflectance spectroscopy is concerned with the materials' light absorption and reflectance properties. Different substances reflect wavelengths of light distinctly differently so that the reflectance characteristic of an object can give some indication of the object's material or at least help to differentiate between two objects that look alike to the human eye.

Hegemann T., BÃijrger F. and Pauli J.
Combined High-Resolution Imaging and Spectroscopy System - A Versatile and Multi-modal Metrology Platform.
DOI: 10.5220/0006134602150222
In *Proceedings of the 5th International Conference on Photonics, Optics and Laser Technology (PHOTOPTICS 2017)*, pages 215-222
ISBN: 978-989-758-223-3

It is possible to differentiate between 1-dimensional and polydimensional measurement techniques. The former denotes a point measurement, also called a whisk broom scanner (Green et al., 1998), in which the full spectral data is obtained for a single point, while the latter applies to line-scan systems, area scanning and snapshot imaging. A line-scan system, also known as a push broom scanner (Weser et al., 2008), is able to acquire the spectral data for one line instead of a single point. For an image with a width of x pixels and a height of y pixels, the push broom scanner obtains spectral data (λ) for every pixel x in one line (y_i) simultaneously. To acquire the whole data cube, the push broom only has to scan each of the y lines, making the method faster than a whisk broom scanner which has to scan $x \times y$ times in order to obtain the whole data cube. However, the push broom scanner is not as versatile as a whisk broom scanner, as the width of the scanning unit is fixed and it is thus not possible to freely choose the part of the sample for which to acquire hyperspectral data. Area scanning, also called spectral scanning (Dickinson et al., 2001), is another technique which allows for surveying the whole image monochromatically, meaning that a value for every pixel of the image is obtained for one certain wavelength λ. This can be achieved either by using a broadband light source and an optical band-pass filter, which rejects all but one wavelength and may be tunable or has to be replaced in order to allow for more wavelengths to be scanned, or alternatively by using a light source with adaptable spectrum. With this technique, it is easy to choose certain spectral bands for the whole image. However, in order to acquire data of several wavelengths, the station has to be stationary, as otherwise spectral smearing can occur, thus deteriorating correlations of an object at multiple wavelengths. Finally, snapshot imaging, also referred to as non-scanning (Volin et al., 2001), is a technique which allows for obtaining the whole data cube at once. This is naturally very time-efficient, but computational effort and initial costs are high.

For the metrology platform presented in this paper, a point scanner was chosen as it is the most versatile of the described techniques and also the most affordable. Due to the positioning robot, which allows for nanometer-exact positioning, a high-resolution spectral image can be obtained for heterogeneous samples. Furthermore, the choice of the characteristics of the spectrometers is flexible and almost any wavelength range can be analyzed. The only drawback is the relatively slow capturing process compared to the other recording approaches.

3 SYSTEM OVERVIEW

Atop of a vibration damped optical table, a three axis Cartesian robot with nanometer-precision and a combined measurement head for large area gray value images as well as spectral measurements is placed. A lighting system encompassing LEDs in different colors and infrared along with an ultraviolet light provides the means to acquire multispectral images, while a broadband halogen light facilitates hyperspectral image acquisition with the aid of spectrometers. An overview of the system's exterior, with the important instruments and parts of CHRISS, as well as the system's main components of the interior, is presented in Figure 1.

3.1 Enclosure

The core of the system is mounted atop the vibration damped optical table manufactured by the Opta GmbH and is surrounded by a light-proof enclosure construction with a canvas hull. Building vibration is a problem when dealing with high-precision image acquisition. In order to handle this problem, a table which absorbs most of the vibration is used, thus ensuring that the measurement of the sample is not corrupted. A granite surface plate manufactured by the company Johann Fischer Aschaffenburg is used as the precise base for transacting measuring and inspection tasks. It guarantees a flatness of the measuring surface according to DIN 876 and is thus important for nanometer-precise measurements.

Additionally, the influence of variable daylight has to be minimized to ensure that measurements of the same sample are always comparable. For that reason the opaque enclosure is important, ensuring that only the internal lighting system illuminates the sample. Since the user has to be able to access the interior to, for example, replace samples, a roller blind has been installed on the front of the canvas hull which can be lowered to make the enclosure light-proof.

Due to the fact that the stages of the Cartesian robot are only guaranteed to operate with nanometer-precision at 20 degrees Celsius, the room is equipped with an air conditioning unit. Since the lighting system, especially the halogen light, causes the air within the enclosure to heat up, a ventilation system interchanging the warm interior and the cool exterior air is necessary to ensure the high-precision work of the positioning robot. A thermometer system with three measuring points provides information about the temperature within the enclosure so that the user is able to assess the precision of the positioning system.

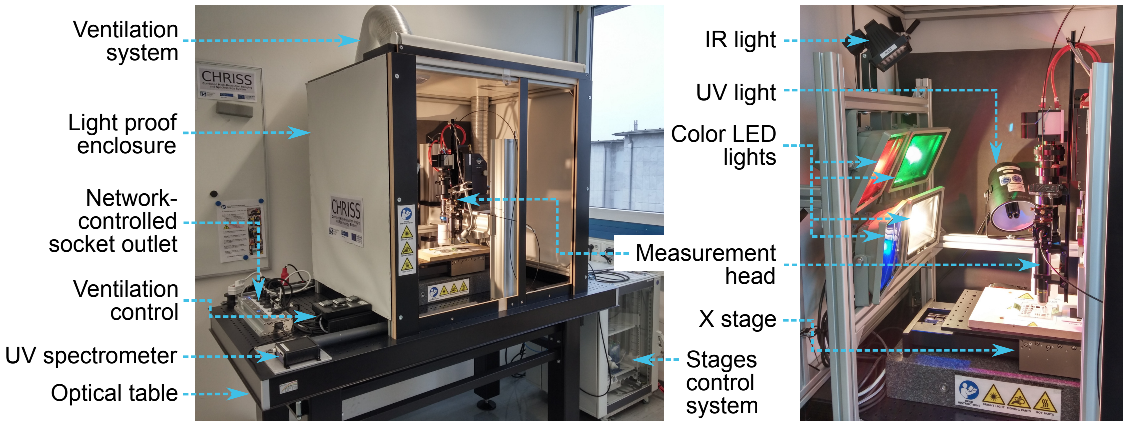

(a) (b)

Figure 1: Overview of the measurement system. Figure (a) shows the exterior of the measurement system. Figure (b) shows the main components of the interior. The NIR spectrometer is not visible, because it is behind the enclosure.

3.2 Cartesian Robot

The Cartesian Robot is equipped with a three-axis high-precision positioning system manufactured by the company Aerotech. The x-stage may carry a high payload of up to $25 kg$ over a distance of $40\ cm$ with a speed of up to $100\ mm/s$. It is an air-bearing linear stage which allows for positioning accuracy of 1 nanometer of samples. On the other hand, the y- and z-stage are connected and hold the measurement head. The y-stage is a cross roller bearing stage and is used to position the measurement head over the region of interest, while the z-stage is an air-bearing linear stage and its position determines the focus of the measurement head with respect to the sample. Since the focal length of both the gray value camera and the spectrometers is fixed, the distance of the measurement head to the sample has to be adjusted to obtain images in focus.

3.3 Illumination System

The illumination system consists of four white LED lights, three of which are equipped with an additional color filter to obtain blue, green and red light. Furthermore an infrared (IR) LED and an ultraviolet (UV) light are installed so that images beyond human vision can be acquired. The illumination system is managed by a network-controlled socket outlet, the *Allnet ALL4076*, so that each light can be switched on and off automatically by the system. Using these six lights and the gray value camera, it is possible to acquire multispectral images by taking one image with the camera for each light source thus obtaining a multispectral image with 6 spectral channels (gray value, blue, green, red, UV and IR). Additionally, a broadband halogen lamp is mounted near the measurement head and moves together with it in order to produce light for the spectrometers. The halogen light offers a broad spectrum of light ranging from approximately $400 nm$ to $1700 nm$, thereby providing light for the majority of the acquirable spectrum, while neglecting the ultraviolet region. The acquisition of a light type more suitable to the task, which ensures that data in the UV region as well as in the visible and near IR spectrum can be obtained, like a confocal broadband fiber optics light source, is planned for the future.

4 MEASUREMENT HEAD

The measurement head is a combined system of camera and spectrometer units in which both units are mounted on rails along the z-axis. The measurement location of camera and spectrometers are distinct because of the offset between camera and spectrometer unit along the y-axis, as can be seen in Figure 2. Since the relative position of camera and spectrometer unit can be calibrated (see section 5.3), it is possible to scan an area first with the camera in order to find the desired section of the sample and then acquire the full spectral range in one or several defined points by means of the spectrometer module. This combination of camera and spectrometer units, along with the high-precision positioning system, offers a versatile approach of scanning large areas with the camera to find regions of interest which can be examined more closely by utilizing the spectrometers.

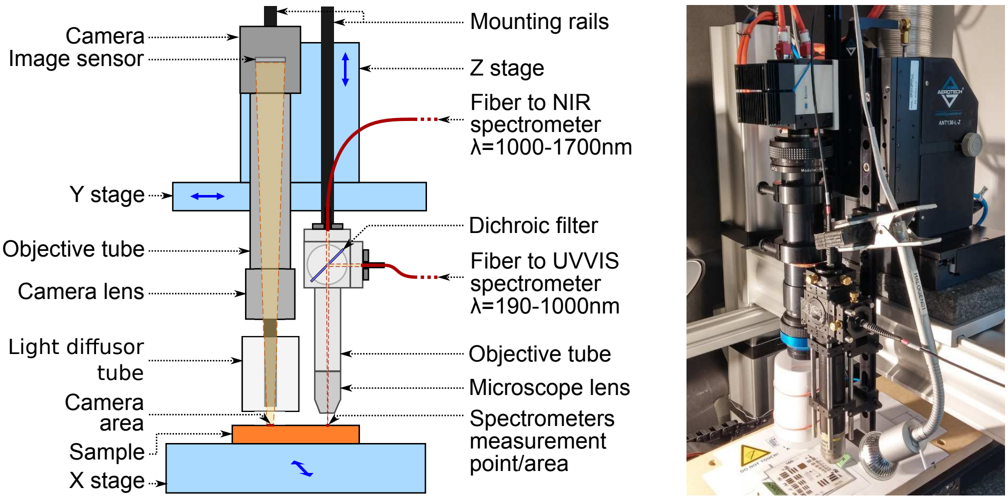

(a) (b)

Figure 2: Detail description of the measurement head. Figure (a) shows the components and the light paths. Figure (b) depicts the actual system with the side-mounted light source for the spectrometers.

4.1 Camera Module

For the camera module, the industrial gray value camera *Baumer SXG80* with a resolution of 3296×2472 pixels (8 megapixel CCD sensor) is used. In combination with the objective *inspect.x L 105mm* manufactured by the company Qioptiq, which allows for 2x magnification while featuring very low optical distortion, it is utilized to obtain high-resolution surface scans of a sample. The camera module is especially applicable when inspecting large samples for defects, as it is used to localize regions of interest. In combination with the illumination system, it is possible to acquire multispectral images with 6 waveband channels, as can be seen in figure 3. Although the camera may only acquire images of a small section of the sample, i.e. approximately 2×2 *cm*, the positioning system in combination with a stitching module facilitates the attainment of large-area images. Image stitching allows for the acquisition of large scale images, but poses the problem of possibly creating visible seams where two images meet. Due to the fact that the camera in CHRISS is not perfectly aligned with the positioning stage, it is necessary to compensate the problem of slightly rotated images by cropping them, thus only using the inner part of the overlapping images. In this way, the stitching module yields large area scans of the surface of the sample without visible seams, which can be seen in Figure 4.

In order to be able to reduce the impact of luminous reflectance and unevenness of samples, a light dispersion unit can be utilized. This unit is placed between camera objective and sample so that light from the light source in use does not directly illuminate the sample but the dispersion unit instead, which provides a uniform light distribution and ensures a diffuse illumination setting. As a consequence, shadows casted by surfaces with 3D structure can be minimized. Thus, images of samples are generally less affected by problems of uneven surfaces and reflections caused by direct illumination of glossy surfaces. To this effect, either a semi-transparent cylindrical dispersion unit for a diffuse bright field or an opaque cylinder for a dark field can be utilized, the results of which can be seen in Figure 5.

4.2 Spectrometer Module

The presented measurement system utilizes reflectance spectroscopy to facilitate a more detailed examination of samples. The spectrometer module consists of two separate spectrometers which are combined in order to acquire a wide range of spectral data for a single point. For the purpose of obtaining data ranging from the near ultraviolet region (190-390 *nm*) to the visible spectrum (390-700 *nm*) up to the beginning of near infrared data (700-1,100 *nm*) the *BaySpec Super Gumet UV-NIR* spectrometer is utilized, while the *BaySpec Super Gamut NIR* spectrometer, with a range of 900 to 1,700 *nm*, is used to extend the examinable scope of IR data. To acquire the full spectrum (190-1,700 *nm*) at one single point, the spectrometers are combined using a dichroic mirror that serves as a filter which reflects light of a certain spectrum while allowing the remaining light to pass through. In this case a dichroic mirror at $\lambda = 1{,}000$ *nm* is used, meaning that light below 1000 *nm* is reflected while light above 1000 *nm* passes the filter unimpeded. From the

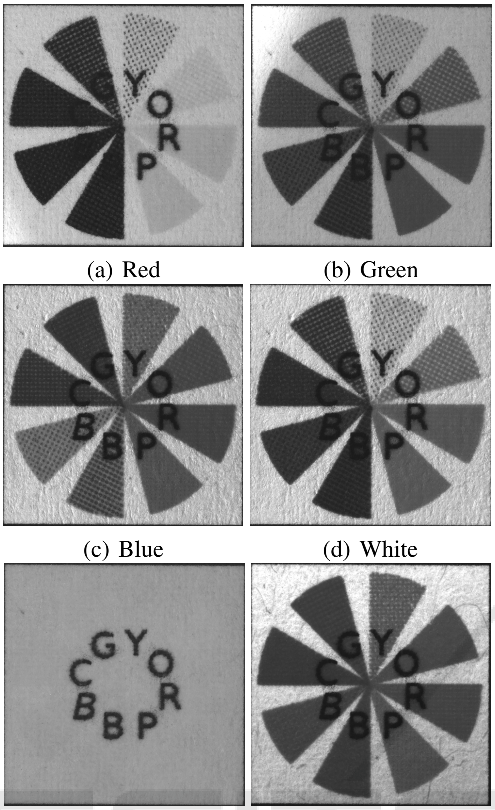

(a) Red (b) Green

(c) Blue (d) White

(e) IR (f) UV

Figure 3: Multispectral image channels with denoted light sources. The sample is a colored calibration pattern printed on paper.

dichroic filter, two fiber optic cables lead to the respective spectrometers where the optical signal is discretized. In this way, it is possible to have two spectrometers acquiring data from nearly the same area, as depicted in Figure 2 (a). In order to minimize the size of the area, thus allowing for more accurate measurements with higher resolution, a microscope lens, namely the *Nikon TU Plan Fluor 10x*, is attached to the end of the objective tube of the spectrometer head. In this way, a point resolution of 60 μm is achieved.

A total of 3,904 measurements can be obtained with the two spectrometers for each sample point, 3,648 of which are conducted by the UV-NIR spectrometer, which amounts to 3.97 measurements per nanometer of the spectral band, while the NIR spectrometer offers an additional 256 measurements with a spectral resolution of 0.32 measurements per nanometer. Even though the resolution of the NIR spectrometer is inferior to the other spectrometer, both of them are important to ensure the applicability of the system to a wide variety of tasks, in particular those for which the IR spectrum is significant, as, for example, in quality inspection of steel surfaces.

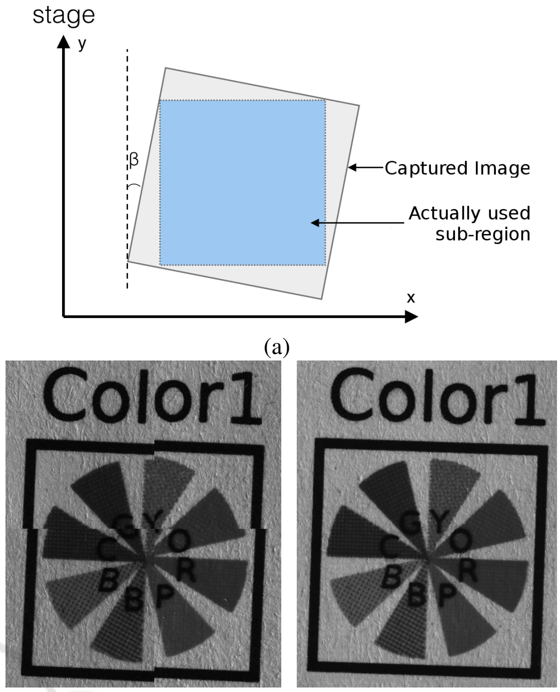

(a)

(b) (c)

Figure 4: (a) Demonstrates the rotation shift between camera and stage. (b) Shows naively stitched image from 4 input images without rotation correction, (c) the result obtained by the presented stitching module with rotation corrections.

5 CAMERA TO SPECTROMETER CALIBRATION

Calibration is a very important topic in the scope of CHRISS. This is due to the fact that the ability to obtain the point spectrum for each pixel in the camera image is desirable. The first aspect of the proposed calibration method is the focus of the camera in order to achieve sharp images. To this effect, an autofocus module has been developed, which is described in

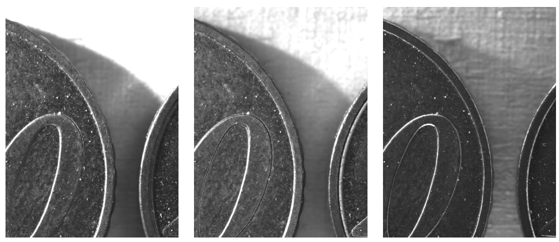

(a) No dispersion (b) Bright field (c) Dark field

Figure 5: Image of reflecting surface with and without dispersion units. Shadows and reflections can be significantly reduced by using bright and dark field. However, more powerful lights are required for the dark field.

section 5.1. Since the spectrometer unit is also an optical device, it needs to be focused as well. Section 5.2 provides the specification of the spectrometer focus. Subsequently, the coordinate system of the spectrometer unit can be calibrated to the camera's coordinate system, in order to obtain the point spectrum for each pixel in the camera image.

5.1 Camera Focusing

In order to obtain camera images in focus, the distance of the camera to the sample is important so that the focal point of the camera coincides with the position of the image plane. Therefore, the camera has to be moved along the z-axis until the focal length concurs with the distance of the image plane to the lens. To be able to automatically evaluate the image focus, an image-based approach has been chosen. A focus metric was implemented based on the Brenner gradient described in (Yazdanfar et al., 2008). The Brenner gradient was extended to obtain a metric in which not only vertical edges are considered but also horizontal edges. The modified Brenner metric B is calculated by

$$B = \sum_{i=1}^{N} \sum_{j=1}^{M} \left(\frac{|s(i-1,j)-s(i+1,j)|+|s(i,j-1)-s(i,j+1)|}{2}\right)^2 ,$$

where $s(i,j)$ is the gray value of pixel (i,j) and N and M are the number of horizontal and vertical pixels respectively. Since an edge in an image induces a significantly higher contrast between neighboring pixels, B increases with more edges in an image and since in-focus images contain more sharp edges, B is accordingly higher for sharp images. The metric B has to be maximized in order to obtain in-focus images and according to (Yazdanfar et al., 2008) a focus function f depending on the vertical position of the camera z can be approximated by a Lorentzian function

$$f(z) = y_0 + \frac{1}{\pi} * \frac{\alpha}{(z-z_0)^2+\alpha^2} ,$$

with α specifying the width, z_0 the center and y_0 the offset of the curve in y-direction.

A hybrid approach for the autofocus of CHRISS has been chosen, which comprises a naive and a curve fitting approach. The naive approach is basically a grid search for the optimal z so that B is maximized. The curve fitting approach is faster but less accurate and works with three images taken from different heights which suffices to fit a Lorentz function to the data points using MSE-minimizing curve fitting. A Lorentzian function has a single maximum at z_0. The z-coordinate corresponds directly to the optimal z-position of the camera to obtain in-focus images. Combining both approaches also combines the advantages, i.e. the approach is faster than the naive grid search but gives more accurate results compared to the curve fitting approach. On average, the camera is positioned within 0.039 *mm* of the optimal z-position in 3.67 seconds.

5.2 Spectrometer Focusing

In order to focus the spectrometer unit, an adaptation of the Brenner-based camera image focus process is proposed. Since the spectrometers do not capture an image but instead just a single "pixel" with almost 4000 different wavelengths, the focusing approach described above cannot be applied without adjustments. However, the principle of examining the sharpness of edges is still valid. The idea is to use a sample pattern with two distinct areas, a black and a white one. After positioning the spectrometer head over the white part of the sample in an initial z position, the measurement head is moved in the y direction, to the black area of the sample. In between, several measurements are carried out so that the intensity value for each waveband and each position on the y-axis is obtained. Using only the wavelength with the highest variation, it is possible to locate the point of transition from white to black by determining the maximum change between two measurements. This is reasonable as it can be assumed that the difference between two measurements is higher for sharp transitions and lower for blurry edges. The spectrometer head is moved in the z-axis after the procedure of finding the maximal intensity difference ΔI_{z_0}, and the next maximal intensity difference is determined. In this way it is possible to find the z-position in which the spectrometer unit delivers sharp measurements by determining the z-position in which the maximum change $\max(\Delta I_{z_n})$ occurs.

Since the measurement system comprises two separate spectrometers and since both of the optical fiber cables were manually positioned and fixated, and are thus not centered perfectly on the optical axis, the focus point of the two spectrometers differs slightly. It is therefore possible to find different optimal z-positions for both spectrometers, however, to allow for faster intensity value acquisition of all wavelengths in one point, the mean value of the two best z-positions is taken as the optimal z_{best}.

5.3 Point Calibration

Point calibration describes the process of finding the same point in a camera image and with the spectrometer unit. This should be possible so that regions of interest, which were found by analyzing the image obtained with the camera, can be examined more closely by means of utilizing the spectrometers. In order to

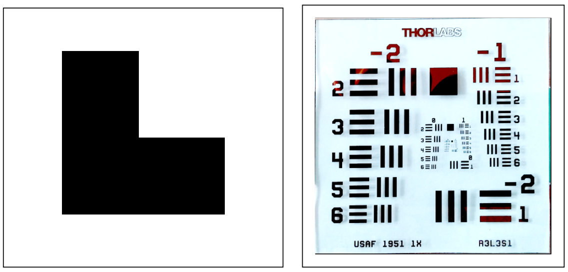

(a) Coarse calibration pattern. (b) Fine calibration pattern.

Figure 6.

find the same point with camera and spectrometers, the coarse calibration pattern, which is shown in Figure 6 (a), is used. It is easily possible to find the corner at the center of the pattern using a regular image, however, since the spectrometers only scan one point at a time, it is a challenging task to find the corner using the spectrometers. In order to do so, the user places the calibration pattern approximately under the spectrometer head and a number of measurements are taken along the *y*-axis for the purpose of finding the horizontal edge, similarly to detecting the edge when focusing the spectrometers. When the *y*-coordinate of the edge is found, the measurement head is moved in the *x*-axis and the process of finding the edge is repeated so that several *y*-coordinates are found corresponding to the horizontal edge. In a respective way several *x*-coordinates are determined for the vertical edge. The intersection point of the two lines obtained in this way corresponds to an approximation of the target corner of the calibration pattern. Since this is only a coarsely estimated target point, it is possible to improve upon the results by taking an array of hyperspectral measurements in the vicinity of the found intersection point, as can be seen in Figure 7 (a). The obtained data can be regarded as a large number of images by considering a single wavelength at a time, thus obtaining a total of 3,904 images. Each image is preprocessed with morphological filters using structuring elements (Efford, 2000). By utilizing a combination of the Canny edge detector (Canny, 1986) and Hough transform (Duda and Hart, 1972), it is possible to find a proper representation of the two perpendicular lines in each image. The intersection of the two lines is determined for each image and the median coordinates of the intersection points are calculated in order to find an accurate representation of the target corner point. To find the exact offset of the camera to the spectrometer head, several more aspects are taken into consideration. It is necessary to find the size of pixels in the camera image to translate a distance in the image coordinate system (CS) to the positioning stage CS and also determine the rotation

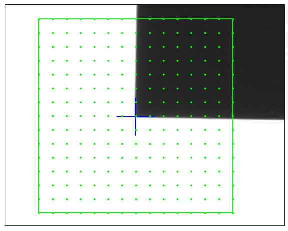

(a)

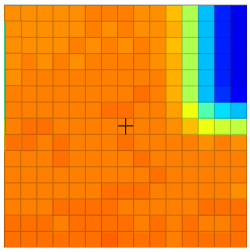

(b)

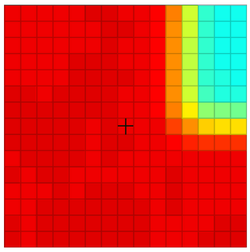

(c)

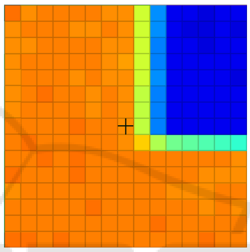

(d)

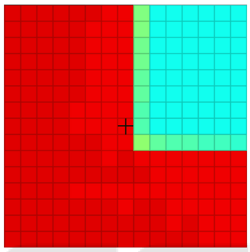

(e)

Figure 7: Calibration results. (a) shows the selected area of the image with green dots indicating spectrometer measurement locations. (b) and (c) reveal the results for UV-NIR and NIR spectrometer respectively after coarse calibration, i.e. blurry lines and corner does not match center point (black plus). (d) and (e) show improved results with sharper lines and lower offset between center and corner for the two spectrometers with wavelengths of 702 *nm* and 1360 *nm* respectively.

between camera and the stage. Since the camera was installed manually, it is not perfectly aligned with the axis of the stage, therefore a rotation parameter has to be found in order to move the stage properly with respect to the information provided by the camera image. It is also necessary to consider that the found intersection point differs for the two spectrometers, as explained above, hence the mean value of the two coordinates of the intersection points is used as an estimate of the corner. To improve the results, a fine calibration pattern[1], cf. see Figure 6 (b), manufactured by means of a laser instead of a printer and thus more precise, is used. The results of calibrating with both patterns can be seen in figure 7. The calibration process takes about 67 minutes both for coarse and fine calibration, but it only has to be done once un-

[1]USAF-1951 Standard Target (T-20).

less the hardware setup of the measurement system is changed. Experiments show that the hyperspectral images reach a lateral resolution of 60 micrometers.

6 CONCLUSIONS

With CHRISS, a unique, flexible and versatile measurement system has been developed which contains a high-resolution camera able to obtain multispectral images, also considers a wide area of wavebands due to the combined spectrometer unit and utilizes a high-precision positioning system which allows for thorough analysis of large samples. The hardware of the attained system was presented in detail, and solutions to the major problems of calibration and focus have been described. Construction and implementation of the CHRISS project is finished in general but can be extended in the future to improve the performance, for example by installing a more suitable light source or by using pinholes at the junction of the spectrometer head and the optical fiber cables of the spectrometers. This would improve the lateral resolution of hyperspectral point measurements, but is only applicable in combination with a more powerful light source as less light is able to reach the fibers and thus the spectrometers.

The system may now be used to acquire multi- or hyperspectral data which can be analyzed. Current projects work on clustering of hyperspectral image data and classification of different materials in multispectral space by means of Convolutional Neural Networks (CNN). The applicability of CNNs to hyperspectral image data and its classification results will be explored in the future in order to create a measurement system that holistically analyzes a large sample, detects regions of interest and is able to examine them more closely to detect anomalies in an otherwise homogeneous sample.

ACKNOWLEDGEMENTS

This work was funded by the European Commission within the Ziel2.NRW programme “NanoMikro +Werkstoffe.NRW”.

REFERENCES

Canny, J. (1986). A computational approach to edge detection. *IEEE Transactions on pattern analysis and machine intelligence*, (6):679–698.

Dickinson, M., Bearman, G., Tille, S., Lansford, R., and Fraser, S. (2001). Multi-spectral imaging and linear unmixing add a whole new dimension to laser scanning fluorescence microscopy. *Biotechniques*, 31(6):1272–1279.

Duda, R. O. and Hart, P. E. (1972). Use of the hough transformation to detect lines and curves in pictures. *Communications of the ACM*, 15(1):11–15.

Efford, N. (2000). *Digital image processing: a practical introduction using java (with CD-ROM)*. Addison-Wesley Longman Publishing Co., Inc.

Green, R. O., Eastwood, M. L., Sarture, C. M., Chrien, T. G., Aronsson, M., Chippendale, B. J., Faust, J. A., Pavri, B. E., Chovit, C. J., Solis, M., et al. (1998). Imaging spectroscopy and the airborne visible/infrared imaging spectrometer (aviris). *Remote Sensing of Environment*, 65(3):227–248.

Kortüm, G. (2012). *Reflectance spectroscopy: principles, methods, applications*. Springer Science & Business Media.

Long, D. A. (1977). Raman spectroscopy. *New York*, pages 1–12.

Panasyuk, S. V., Yang, S., Faller, D. V., Ngo, D., Lew, R. A., Freeman, J. E., and Rogers, A. E. (2007). Medical hyperspectral imaging to facilitate residual tumor identification during surgery. *Cancer biology & therapy*, 6(3):439–446.

Radziemski, L. J. and Cremers, D. A. (2006). *Handbook of Laser Induced Breakdown Spectroscopy*. John Wiley & Sons, West Sussex, England.

Skoog, D. A. and West, D. M. (1980). *Principles of instrumental analysis*, volume 158. Saunders College Philadelphia.

Volin, C. E., Garcia, J. P., Dereniak, E. L., Descour, M. R., Hamilton, T., and McMillan, R. (2001). Midwave-infrared snapshot imaging spectrometer. *Applied optics*, 40(25):4501–4506.

Weser, T., Rottensteiner, F., Willneff, J., Poon, J., and Fraser, C. S. (2008). Development and testing of a generic sensor model for pushbroom satellite imagery. *The Photogrammetric Record*, 23(123):255–274.

Yazdanfar, S., Kenny, K. B., Tasimi, K., Corwin, A. D., Dixon, E. L., and Filkins, R. J. (2008). Simple and robust image-based autofocusing for digital microscopy. *Opt. Express*, 16(12):8670–8677.